Essential Readings in Light Metals: Electrode Technology for Aluminum Production.
Edited by Alan Tomsett and John Johnson.

EXTRINSIC AND INTRINSIC ASPECTS OF ANODE CRACKING

Tianshun Liu
Advanced Materials Program, Australian Nuclear Science and Technology Organisation, Private Mail Bag 1, Menai, Australia 2234

Les C. Edwards, Colin P. Hughes and Brendan J. Mason
Comalco Research Centre, P.O. Box 316, Thomastown, Australia 3074

Robert McMellon,
Boyne Smelters Limited, Handley Drv., Gladstone, Australia 4680

Abstract

The cause of anode cracking at an operating smelter has been investigated by determining the influence of plant parameters (extrinsic factors) on anode cracking and by studying the intrinsic properties of the carbon to determine its susceptibility to thermal shock cracking.

The major cause of anode cracking was found to be the *propagation of pre-existing* baked cracks. Detailed mechanical property tests indicated a limited amount of non-linear inelastic behaviour, characteristic of a brittle material. For the particular cracking problem experienced, resistance to crack propagation was found to be more critical than resistance to crack initiation. Using the mechanical properties and thermal stress modelling, the critical flaw size above which a crack will propagate was calculated to be 50 mm. The paper highlights the importance of understanding the nature of anode cracking and the influence of both extrinsic and intrinsic factors.

Introduction

Cracking of anodes during cell operation is often attributed to the severe thermal stress that anodes are subjected to when first placed in the cell[1-5]. At the particular smelter under investigation, an increase in anode cracking (as measured by increased unscheduled anode changes) coincided with an increase in anode size. Process changes were implemented which reduced anode unscheduled changes to historical levels. However, extensive testing as detailed later in this paper, suggests the properties of the anode are such that the anode is still susceptible to thermal shock. This is most apparent from the number of butts which return from the cell with some vertical transverse or longitudinal cracks (Figure 1).

Following a detailed audit of the plant in 1992 by an outside consultant, it was suggested that the main cause of cracking was due to the low and variable flexural strength of the anode carbon. This was attributed to variation in the sizing of the aggregate fractions, particularly the fines fraction. A plant study was undertaken to assess the sources and level of variation in the plant to determine which areas were contributing significantly to anode cracking. The level of anode cracking was determined by measuring and characterising the cracks in the returned butts.

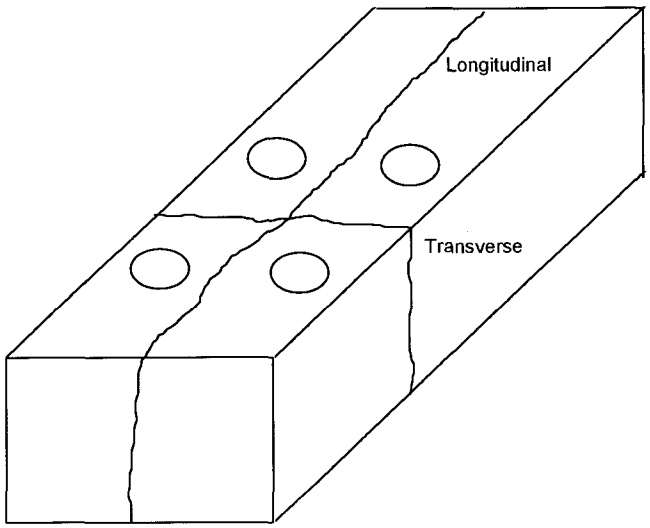

Figure 1: Vertical crack orientation.

In addition extensive testing of the mechanical and thermal shock properties of the anode carbon was undertaken to determine the intrinsic thermal shock resistance of the carbon. Plant studies had found that a significant number of anodes developed vertical transverse and longitudinal cracks across the base shortly after setting in the cell.

This paper presents the findings of the study and discusses them in terms of intrinsic and extrinsic factors that affect anode cracking. Intrinsic factors refer to the material response to a thermal stress field, ie. the behaviour of crack initiation and propagation as well as the crack stability under thermal shock. Such behaviour is related to the microstructure of the anode and the mechanical, thermal and thermal shock properties of the material (Figure 2).

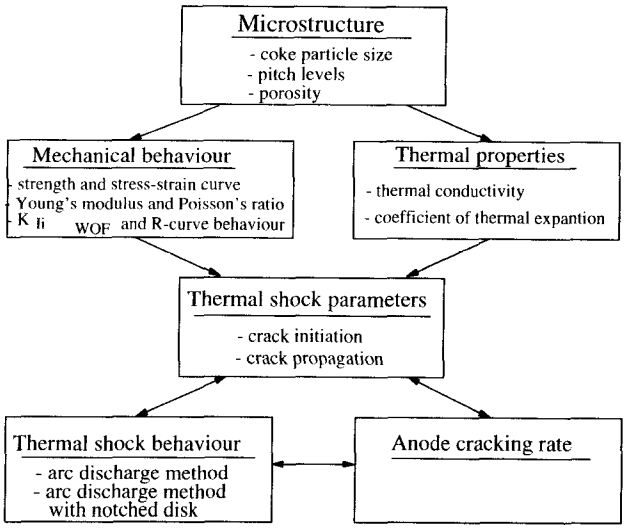

Figure 2: Intrinsic aspects of anode cracking.

Extrinsic factors deal with the driving force for anode cracking (Figure 3). The thermal stress field is determined by many factors such as the size of the anodes, stub and yoke design, potline operation and some intrinsic material properties. Anode processing may also introduce cracks into the baked material which may be considered extrinsic factors. The thermal stress field and the presence of cracks determine the thermal stress intensity factor, $K_{I,thermal}$, which represents the driving force for anode cracking. A critical crack size above which a crack will propagate when the anode is placed in the cell can be determined.

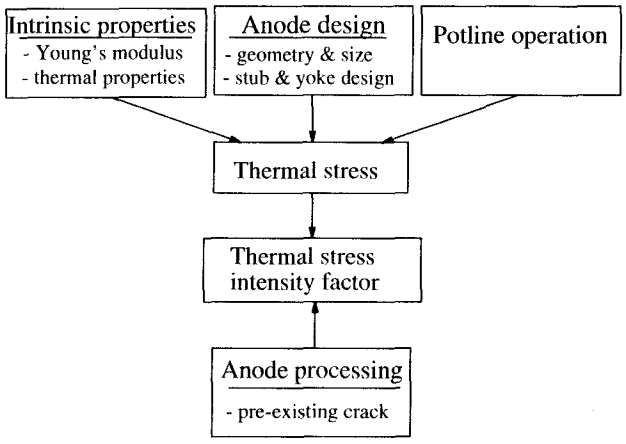

Figure 3: Extrinsic aspects of anode cracking

Plant Study

The anode production process was monitored and samples taken over a six week period. A schematic of the experimental program is shown in Figure 4. Each experimental run involved tracking a batch of material through the process, taking samples and monitoring the production data. Fines, coarse, butts and green scrap fractions were representatively sampled at the exit from the storage bins. The samples were sized and the Blaine Index measured on the fines sample. The blended aggregate was then tracked through the pre-heater and mixers to the anode former. Three representative anodes were then set aside. Seventy runs were completed over a three week period resulting in a total sample of 210 anodes.

The green anodes were cored (50 and 100 mm diameter cores) and tracked through the baking furnaces, after which they were cored again. They were then tracked through potrooms and the returned butts inspected for cracking and airburn. Production data in green carbon, baking and potrooms were collected for all anodes.

Anode Property Testing

The following tests were performed on the baked cores:

baked anode density
electrical resistivity
thermal conductivity
air permeability
air reactivity
flexural strength (3 pt and 4 pt bending)
fracture energy (3 pt bending, notched sample)
biaxial strength
compact tension

The latter three tests are described briefly below:

Fracture Energy

Fracture energy is a measure of the resistance to crack propagation of the material. Fracture energy tests were conducted on 50 mm diameter cores. The span width was 100 mm. A Chevron "V" notch of angle 60° was cut in the mid-point of the core to a depth of 10 mm. The fracture energy was determined by calculating the area under the load/displacement curve to the break-point.

Biaxial Strength

Biaxial strength is one of a number of methods of determining material strength. Biaxial strength tests were conducted on 100 mm diameter disks, 10 mm in thickness. The loading rate was 0.01 mm/sec. The strength σ_{max} was determined by the following equation[6]:

$$\sigma_{max} = \frac{3P_{max}(1+\nu)}{4\pi t^2}\left[1 + 2\ln\frac{A}{B} + \left(\frac{1-\nu}{1+\nu}\right)\left(1 - \frac{B^2}{2A^2}\right)\frac{A^2}{R^2}\right] \quad (1)$$

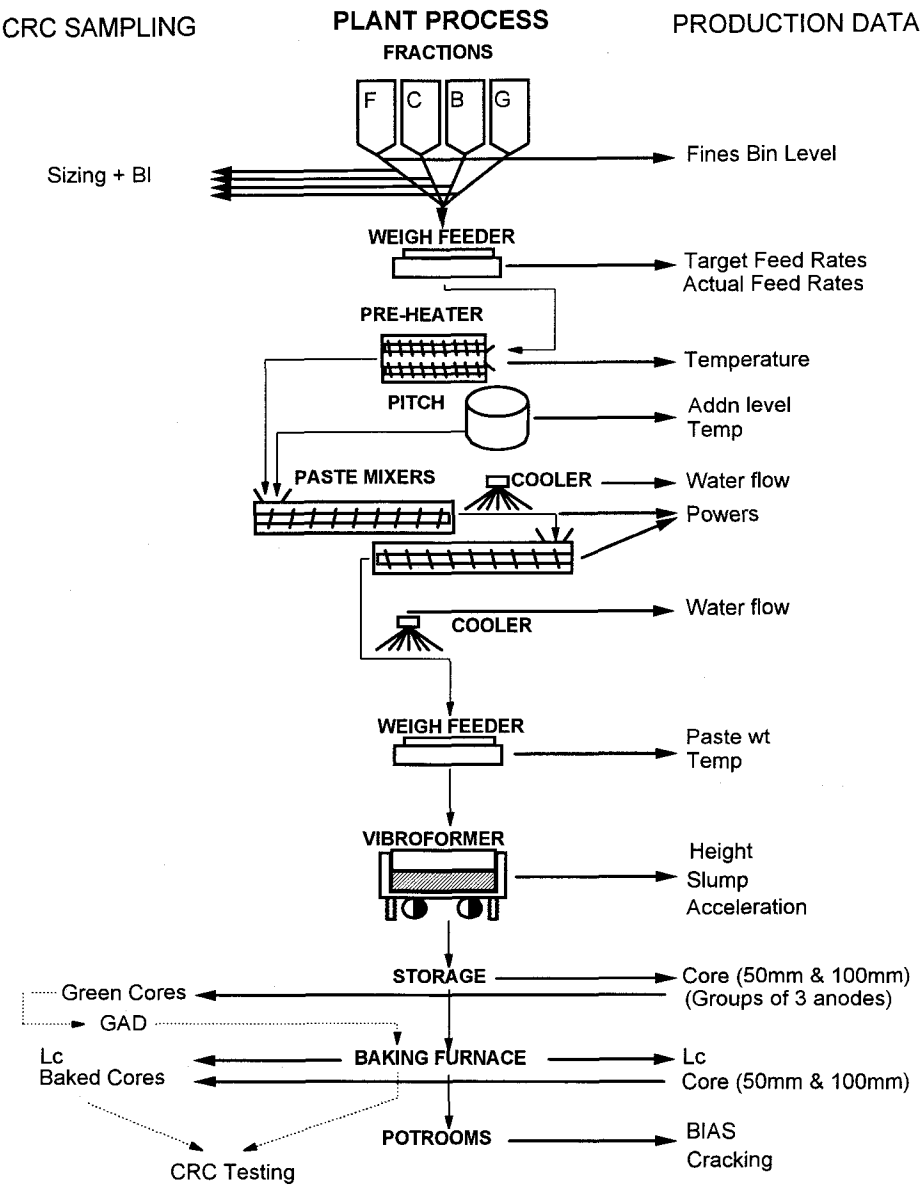

Figure 4: Schematic of experimental program.

where P_{max} is maximum load, ν is Poisson's ratio, A is radius of the support ring (=38 mm), B is radius of the upper loading flat (=12.7 mm), R is radius of the disk (=50 mm) and t is thickness of the disk (=10 mm).

Compact Tension

Compact tension tests were also conducted on 100 mm diameter disks, 10 mm in thickness. The test is shown schematically in Figure 5. The distance w was 74 mm. The ratio a/w was kept constant at 0.5. The notch width was 0.25 mm. Tests were conducted in position control with a speed of 0.005 mm/sec. An extensometer with a range of 2.5 mm was used to measure the Crack Mouth Opening Displacement (CMOD).

Load versus CMOD curves were recorded using an x-y chart recorder. The work of fracture γ_{WOF} was calculated using the following equation:

$$\gamma_{WOF} = \frac{U_T}{2A_1} = \frac{1}{2t\Delta a}\int_0^f P\,df \qquad (2)$$

where U_T is total energy, A_1 is area of the fracture surface, Δa is crack extension, P is load and f is load-point displacement. The critical stress intensity factor to initiate crack growth K_{Ii} was calculated by[7]:

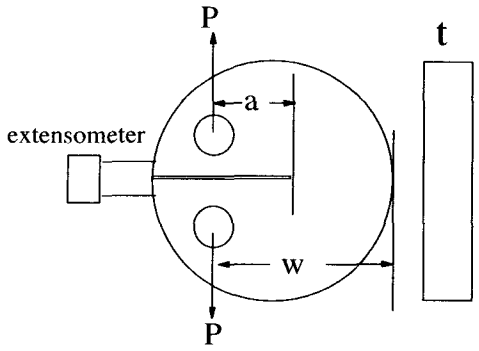

Figure 5: Schematic of compact tension test.

$$K_{Ii} = \frac{2P_{max}\alpha f(\alpha)}{t\sqrt{w(1-\alpha^{1.5})}} \quad (3)$$

where $\alpha = a/w$ and

$$f(\alpha) = 0.76 + 4.8\alpha - 11.58\alpha^2 + 11.43\alpha^3 - 4.08\alpha^4 \quad (4)$$

The fracture energy for crack initiation γ_i was calculated as follows:

$$\gamma_i = \frac{K_{Ii}^2(1-\nu^2)}{2E} \quad (5)$$

where E is Young's Modulus.

Thermal shock parameters were determined from the mechanical properties as described elsewhere in these proceedings[8].

Data Analysis

All of the production data and anode properties were entered into a SAS statistical data base. A total of 25,000 data points were collected. The production data and anode properties were analysed separately in terms of their association with anode cracking. Given the high level of interaction expected within the production factors and the anode properties, an incremental discriminant analysis was performed on each data set to test for multiple effects. A significance level of 85% was used.

Production Factors

The major production factors found to be associated with anode cracking were as follows:

- fines consistency, ie. variation in fines sizing
- mixer power (continuous mixer)
- paste forming temperature
- vibroforming, specifically the cover-weight acceleration
- position of anode in baking furnace
- stall position

The above factors accounted for 80% of the anode cracking observed. The relative contribution of each factor to anode cracking is shown in Figure 6. The significance of these factors is described further in the discussion section.

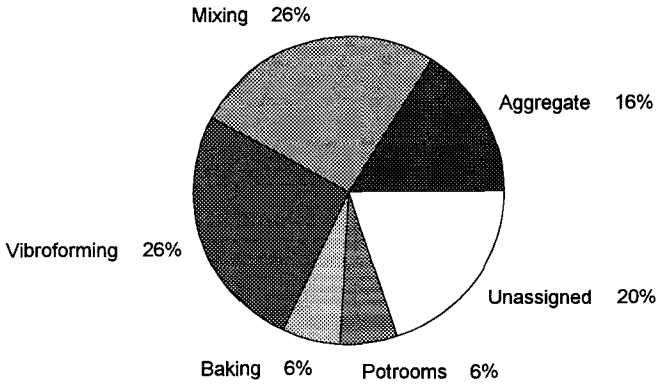

Figure 6: Contributions of production factors to anode cracking.

Intrinsic Factors

Three types of typical stress-strain curves from the four point bending test are shown in Figure 7. Figure 7a represents totally linear-elastic behaviour (OA) whereas some non-linear inelastic behaviour is apparent in Figure 7b,c (AB and ABC). The segment BC is due to the sample breaking within the gauge length (=50 mm). In general the extent of non-linear inelastic behaviour of the anode carbon is very limited, which is characteristic of a brittle material.

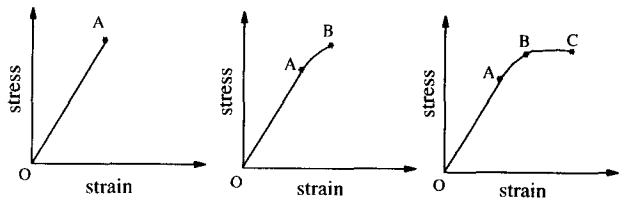

(a) 4PB test: 39% (b) 4PB test: 17% (c) 4PB test: 44%

Figure 7: Typical stress-strain curves from four point bending test.

The only measured anode properties found to be associated with anode cracking were:

- Young's Modulus
- Fracture Energy

Reduced anode cracking was found to occur at lower Young's Modulus and higher fracture energy. This agrees with previous findings[1,5]. The thermal stress experienced by the anode in the cell is directly proportional to Young's Modulus and fracture energy describes the resistance to crack propagation of the anode carbon.

The small number of properties found to correlate with anode cracking was surprising given the initial supposition that cracking was related to some intrinsic property of the anode carbon. One feature which was noted during removal of the core samples from the anode was the frequency with which the core samples were cracked. This suggested that the baked anodes contained a large number of pre-existing cracks.

Extrinsic Factors

The incidence of pre-existing cracks in the anodes was investigated by cutting twenty baked anodes into nine pieces and examining the pieces for cracks. The cutting plan is shown in Figure 8. Fifty percent of the anodes were found to contain significant transverse vertical cracks and 80% were found to contain significant longitudinal vertical cracks. Sufficient cracks were observed to explain the butt cracking incidence. Five green anodes were also cut and no evidence of vertical transverse cracks was found. The cracks appeared to be opening up in the baking process.

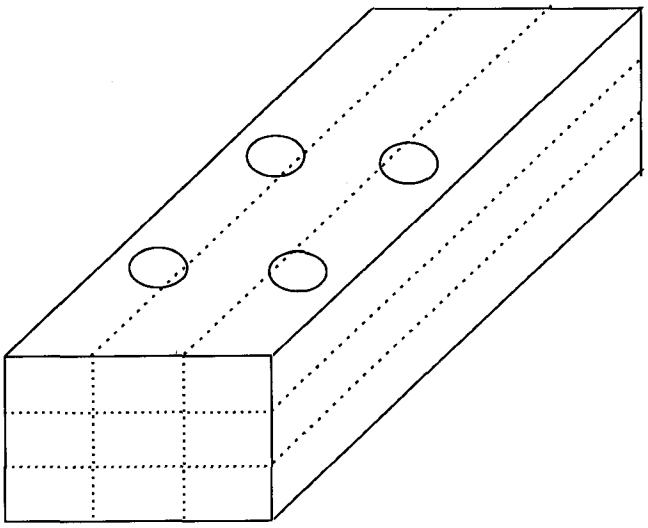

Figure 8: Anode cutting plan.

The propagation behaviour of these cracks after anode setting in the cell was determined by calculating the thermal stress intensity factor, $K_{I,thermal}$. To begin with, the thermal stress experienced by the anode was modelled by finite element analysis using the mechanical properties previously determined[3]. The resultant thermal stress is shown in Figure 9 as a function of distance from the bottom of the anode.

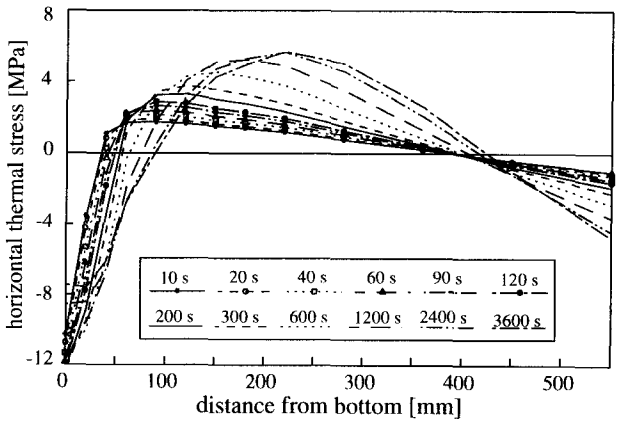

Figure 9: Thermal stress as a function of distance from the bottom of the anode.

Using the modelled thermal stress, the thermal stress intensity factor for a particular crack type/stress field was calculated. This was then used to determine the critical crack size above which a pre-existing crack will propagate when the anode is set in the cell. Two different models of the crack type and stress field were investigated (Figure 10).

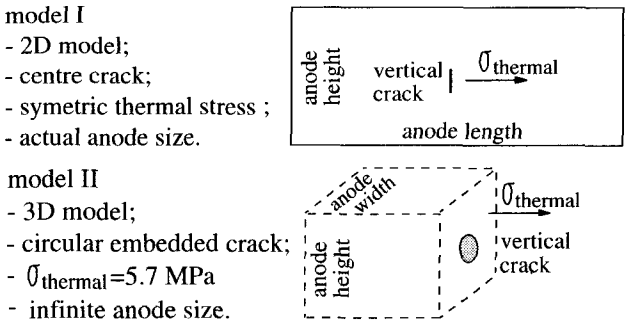

Figure 10: Models of crack type and stress field.

Model I is a two dimensional representation of the anode and assumes a symmetric thermal stress about half the anode height. Model II is a three dimensional model and assumes a constant thermal stress of 5.7 MPa, the maximum value from Figure 9. The calculation of $K_{I,thermal}$ for the 3D case was simplified by assuming an infinite anode size.

The thermal stress intensity factors for both models were calculated as follows:

Model I:

$$K_{I,thermal} = \int_0^a \sigma_{thermal}(y) m(a,y) \mathrm{d}y \qquad (6)$$

Model II:

$$K_{I,thermal} = \frac{2}{\pi}\sigma_{thermal}\sqrt{\pi a} \qquad (7)$$

where a is crack length, $\sigma_{thermal}$ is the thermal stress in the horizontal direction and $m(a,y)$ is the weight function[9,10].

The thermal stress intensity factors for Models I and II are shown in Figure 11 as a function of crack length. The $K_{I,thermal}$ values are higher for the 2D model than for the 3D model. The fracture toughness of the anode carbon was determined from mechanical testing to be approximately 1 MPa$\sqrt{m}$. From Figure 11, the critical crack size for crack propagation in the anode is approximately 20 mm for the 2D model and approximately 50 mm for the 3D model. The 3D model is a more realistic representation of the cracking process. Therefore, pre-existing cracks in the baked anodes of length greater than 50 mm are predicted to propagate through the anode after setting. Most of the pre-existing cracks observed when the anodes were cut were greater than 100 mm in length.

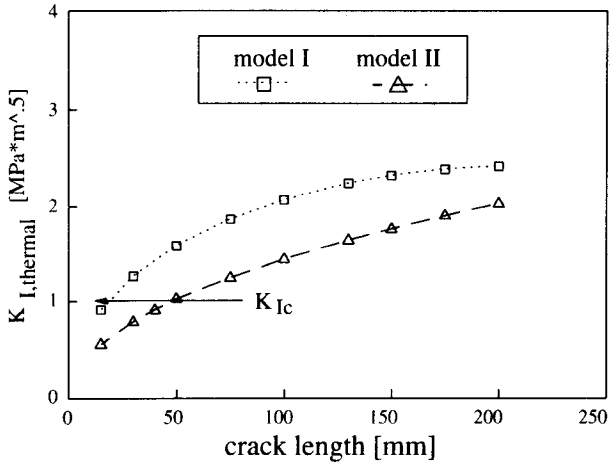

Figure 11: Thermal stress intensity factors for models I and II.

Discussion

The work undertaken indicates that the principle cause of the high anode cracking rate at the smelter is due to propagation of pre-existing internal cracks during the anode rota. The elimination of these pre-existing cracks is part of the ongoing work program and the plant study has highlighted areas which require immediate attention.

Density measurements of cores removed from green anodes indicate there is a marked density gradient through the green anode. In some anodes the density decreases uniformly from top to bottom whereas in others maximum density is observed in the middle (Figure 12, standard paste forming temperature). Lowest densities usually occur at the bottom.

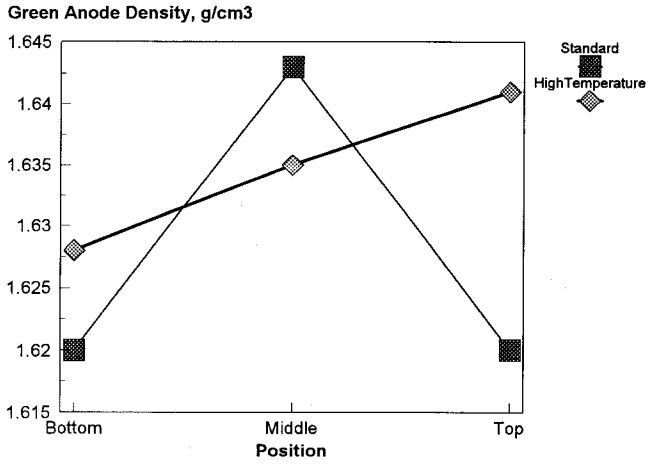

Figure 12: Effect of paste forming temperature on green anode density profile.

The large density profile in the green anode leads to differential shrinkage and expansion stresses during baking. Cracks will move from low density to high density regions. Many cracks in the baked anodes appear to have propagated upwards from the bottom.

A number of the green carbon factors found to correlate with anode cracking impact directly on green anode density profiling. Significant variation was found in the fines fraction (Blaine Index average = 3100, standard deviation (s.d.) = 530) and mixer power (av. = 107 kW, s.d. = 6 kW). This variation is likely to result in variable density in the anodes. Improved ball mill control and automated mixer power control are currently being implemented at the plant.

Cracking was found to be reduced with increased mixer power, paste forming temperature and vibroformer cover-weight acceleration. The impact of an increase in paste forming temperature on the green anode density profile is shown in Figure 12. Some care must be taken with this approach however as excessively high forming temperatures have been found to increase horizontal cracking in green anodes[11]. Increases in mixer power and vibroformer cover-weight acceleration would also be expected to result in better paste homogeneity and compaction and therefore reduced green density profiles.

Anodes in the top layer of the baking furnace and adjacent to the fireshaft also experienced a lower cracking rate. In vertical flue baking furnaces, top layer anodes typically

experience higher but not excessive heat-up rates during preheat. It is possible that bottom and middle layer anode temperatures were still in the critical volatile evolution range when the section went under fire. This could have resulted in these anodes experiencing excessive heat-up rates in this temperature range leading to further cracking due to volatile outgassing.

A small but significant contribution from potrooms to the cracking problem was also found. Anodes set in corner stalls experienced a lower cracking rate. Bath freeze melting is believed to be slower in the corner stalls due to the proximity to pot ledges, thus resulting in lower thermal shock stresses.

The current anode cracking problem is therefore dominated by extrinsic factors (pre-existing baked cracks) rather than the intrinsic properties of the anode carbon. Although the propagation of cracks at BSL is due to the application of a thermal stress or thermal shock, it is perhaps inappropriate to describe the problem as one of thermal shock cracking.

The study has highlighted the importance of considering the crack propagation behaviour of carbon anode materials when investigating anode cracking problems. Given the large mass of an anode it is unrealistic that all anodes will be free of large internal flaws or cracks. Improvements in crack propagation resistance rather than crack initiation are therefore important and strategies to address this issue are discussed elsewhere[8].

Conclusion

The major cause of anode cracking at a smelter has been identified as the propagation of pre-existing internal cracks. These cracks appear to be forming during the baking process as a result of density gradients in the green anodes. The critical flaw size above which a crack will propagate after anode setting in the cell was calculated to be 50 mm. Resistance to crack propagation is therefore of more importance than resistance to crack initiation for this particular cracking problem. It is necessary to examine the role of both extrinsic and intrinsic factors when dealing with anode cracking.

References

1. E. Kummer and W. Schmidt-Hatting, "Thermal Shock in Anodes for the Electrolytic Production of Aluminium," Light Metals, 1990, 485-491.

2. J. Bigot, "Study of Anode Manufacturing Parameters Influencing the Thermal Shock Resistance," Light Metals, 1990, 493-496.

3. P.S. Cook, "Finite Element Modelling of Thermal Stress in Anodes," Light Metals, 1993, 603-609.

4. J.P. Schneider and B. Coste, "Thermomechanical Modelling of Thermal Shock in Anodes," Light Metals, 1993, 621-628.

5. M.W. Meier, W.K. Fischer, R.C. Perruchoud and L.J. Gauckler, "Thermal Shock of Anodes - A Solved Problem?" Light Metals, 1994, 685-694.

6. R. Thiruvengadaswamy and R.O. Scattergood, "Biaxial Flexural Testing of Brittle Materials," Scripta Metallurgica et Materialia, 25, 1991, 2529-2532.

7. J.C. Newman, Jr., "Stress Intensity Factor and Crack Opening Displacements for Round Compact Specimens," Int. J. Fracture, 17, 1981.

8. T. Liu, P.S. Cook, C.P. Hughes and B.J. Mason, "Thermal Shock Crack Initiation and Propagation Behaviour of Carbon Anodes," Light Metals, 1995.

9. A.F. Emery, G.E. Walker, Jr. and J.A. Williams, "A Green's Function for the Stress-Intensity Factors of Edge Cracks and Its Application to Thermal Stress," J. Basic Eng., n12, 1969, 618-624.

10. X.R. Wu and X.G. Chen, "Wide-Range Weight Function for Centre Cracks," Eng. Frac. Mech., 33, n6, 1989, 877-886.

11. R. Lillingston, "Green Anode Flaw Investigations," Internal Plant Report.